

PHYSICAL REVIEW B

CONDENSED MATTER

THIRD SERIES, VOLUME 46, NUMBER 24

15 DECEMBER 1992-II

X-ray-absorption-spectroscopy studies of transition-metal–boron compounds

J. Chen and M. Croft

Department of Physics and Astronomy, Rutgers University, Piscataway, New Jersey 08855

Y. Jeon

Applied Physical Sciences Division, Brookhaven National Laboratory, Upton, New York 11973

X. Xu and S. A. Shaheen

Department of Physics, Center for Materials Research, Florida State University, Tallahassee, Florida 32306

F. Lu

University of Kentucky, Lexington, Kentucky 40506

(Received 11 May 1992)

$L_{2,3}$ -edge x-ray-absorption-spectroscopy studies of the white-line feature are used to probe the electronic structure of $4d$ transition-metal (T)-based materials. Results of such probes of the elements Mo to Ag are reviewed. Results of a number of binary Pd-B and ternary Rh-B compounds are interpreted in terms of the loss of d states just above E_F and the formation of hybridized T - $4d$ /B antibonding states split well above E_f .

INTRODUCTION

Understanding the electronic structure of transition-metal (T) compounds must invariably be grounded on an understanding of the role of the T - d orbitals. In recent years near-edge T - $L_{2,3}$ x-ray-absorption-spectroscopy (XAS) measurements have emerged as a powerful probe to selectively study these important T - d orbital states. These studies focus on the strength and structure of the “white-line” (WL) $2p \rightarrow d$ transition feature that dominates the $L_{2,3}$ near-edge landscape.^{1–13} Specifically, the WL feature intensity has been used to estimate the number of d -orbital holes and bonding-induced changes in this hole count in both $5d$ (Refs. 7–9) and $4d$ (Refs. 10–13) row compounds. In this paper we will first review a systematic WL study of the latter $4d$ elements and then use this XAS method to investigate the T - d orbital electronic structure changes in response to varying B content in a series of T - $4d$, boride compounds [$\text{Pd}_{1-x}\text{B}_x$; PrRh_3B_n ($n=0,1,2$)]. The results will be interpreted in terms of the depletion of d states at E_F and the formation of T - $4d$ /B antibonding states at higher energies.

Transition-metal insertion compounds are a diverse class of materials in which small adatoms are inserted (often continuously) into the interstitial holes of a host crystal structure (e.g., $\text{Pd}_{1-x}\text{H}_x$).^{14–19} In many cases the host lattice remains the same (with a dilation, of course);

however, in others a structural change is induced.¹⁹ Electronically such materials have often been discussed in terms of adatom electron donation directly to the transition-metal d orbitals.^{14–16} However, more recent work has indicated that the introduction of new bonding and antibonding adatom and T - d states well away from E_F can also occur in such materials.^{17,18} Indeed the change of crystal structure in some of these materials is related to the formation of local structures that better exploit this bonding interaction. In this paper a viewpoint will be taken in which some intermetallic compounds with different crystal structures will be considered as extensions of insertion compounds. Specifically Pd_3B , Pd_5B_2 , and Pd_3B_2 will be treated as extensions of $\text{Pd}_{1-x}\text{B}_x$, $x < 0.12$, and PrRh_3B_2 as an extension of PrRh_3B_x , $x < 1.0$.

EXPERIMENT

The compound samples were prepared by standard argon arc furnace techniques. X-ray powder-diffraction measurements were used to verify the proper crystal structure for the various compounds. The XAS measurements were made on beam line X-19A at the Brookhaven National Synchrotron Light Source using a Si (111) double crystal monochromator. The absorption measurements were made in the total electron yield mode to minimize finite-thickness effects.²⁰

WL FEATURE—*d*-STATE CONNECTION

As noted in the Introduction, the WL feature at the $L_{2,3}$ edges of transition metals can provide a powerful probe of the important *d*-character states in solids. In Fig. 1 we show the results (from a recent study²¹) of the L_3 spectra for the $4d$ row elements from Mo to Ag (excepting the radioactive Tc). The zero of energy is set at the inflection point of the edge. As discussed at length previously,⁷⁻⁹ the background before the edge is subtracted from all spectra and the continuum onset step feature at the edge is normalized to unity. The value of the continuum step is determined by the average absorption value near 40 eV (i.e., beyond the WL).

It should be noted that the strength of the WL feature grows dramatically and monotonically from zero at Ag (where the *d*-hole count is essentially zero) to a maximum at Mo. After the method used in $5d$ row XAS studies we have used the Ag spectra as an empirical estimate of the continuum onset and have subtracted the Ag-background spectrum from each of the other spectra to extract the WL feature only. We have then calculated the area of this WL feature between about -3 and $+5$ to $+8$ eV. These WL areas for both the $T(4d)$ L_2 and L_3 edges are plotted in the inset of Fig. 1 versus atomic number. The results of a linear fit to the data is also shown as a solid line.

Elementary chemistry and detailed electronic structure calculations both predict changes in the *d*-hole count between successive $4d$ elements that are close to unity.²³ Indeed any deviations from the natural assumption that this value is unity are beyond the ability of our WL area method to discern. Thus under this assumption the slope of the solid line ($3.6 \pm 0.2 \text{ eV}^{-1}$) represents the expected WL area change for a $4d$ hole count change of one. This rate of WL area change per *d* hole will be used below to estimate changes in the hole count of Pd upon

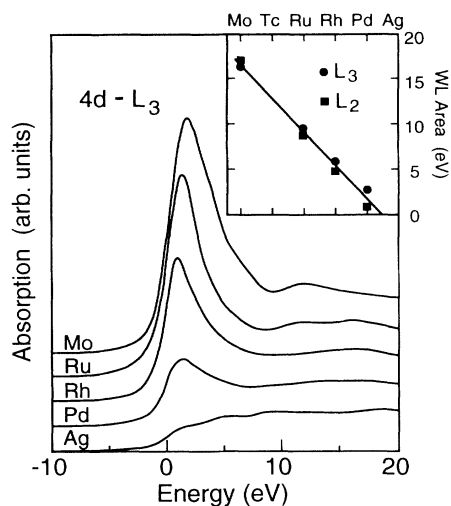


FIG. 1. Elemental $4d$ row L_3 spectra illustrating the growth of the WL feature with increasing $4d$ -hole count. Inset, $T(4d)$ - L_2 and L_3 WL areas vs atomic number illustrating the proportionality of the *d*-hole count to WL area.

alloying with B. It should be noted that while the relative L_2 and L_3 WL area variations can be used to address spin-orbit effects, previous work has indicated that the use of a simple arithmetic average between the L_2 and L_3 WL areas is useful in estimating the net hole count variations. It is this average area method that we will use below.

Pd_{1-x}B_x COMPOUNDS

The decrease in the magnetic response and electronic specific heat of Pd upon "electron addition" via Pd_{1-x}H_x or Pd_{1-x}B_x interstitial alloy formation has been known for many years.¹⁴⁻¹⁸ The filling of the Pd- $4d$ band has

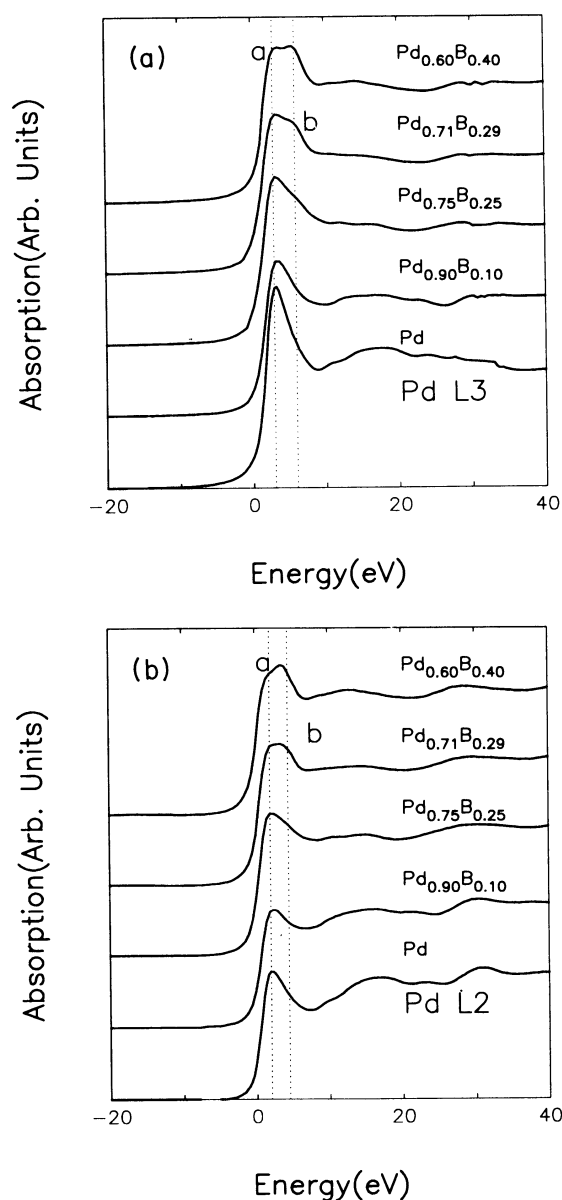


FIG. 2. Pd L_3 (a) and L_2 (b) spectra for Pd, the interstitial alloy Pd_{0.9}B_{0.1}, and the compounds Pd_{1-x}B_x, $x=0.25$, 0.29 , and 0.4 .

been proposed as driving this effect. The series of $\text{Pd}_{1-x}\text{B}_x$ materials with $x=0, 0.1, 0.25$ (Pd_3B), 0.29 (Pd_5B_2), and 0.4 (Pd_3B_2) will be studied here. Only the $x=0.1$ material in this series is a true interstitial alloy of Pd, with the other structures being orthorhombic similar to Fe_3C for Pd_3B , monoclinic similar to Mn_5C for Pd_5B_2 , and hexagonal for Pd_3B_2 .²²

In Fig. 2(a) L_2 and in Fig. 2(b) L_3 spectra of these $\text{Pd}_{1-x}\text{B}_x$ materials are presented. In all of these spectra the zero of energy has been set at the first inflection point, the normalization is set to unity at 40 eV above the edge, and the WL feature is the peaked structure between -5 and $+10$ eV. A number of observations can readily be made from the figures. Upon the increase of B content there is a systematic decrease in intensity of the portion of the WL feature closest to the edge onset [see the region labeled (a) in the figures]. This feature is due to the Pd- d states in the intermediate vicinity above the Fermi energy.

In order to highlight the a feature, spectral changes upon B alloying, we show in Fig. 3 the difference of the $x=0.1$ and 0.0 Pd L_3 spectra. (The $x=0.4$ difference spectrum will be discussed below.) The negative value of the difference spectrum in the WL region reflects the loss of the a feature intensity upon B alloying. Integrating the difference spectra for both the L_3 and L_2 (not shown) edges over the WL range (about -2 to $+7$ eV) yields areas -1.3 and -0.2 eV, respectively, and the average of these area changes $\Delta A = -0.75$ eV. (The continuum step height has been normalized to unity, yielding area units of eV.) Recall the results of the elemental $4d$ WL study above (see Fig. 1) in which a WL area change of 3.6 eV per unity change in $4d$ electron count was observed. Using this WL-area electron-count calibration, the ob-

served $\Delta A = -0.75$ corresponds to about a 0.2 electron increase in d count upon $x=0.1$ substitution or to about 2 electrons donated to the Pd- d orbitals per B interstitial.

Interestingly, in Ce-valence-instability studies of a group of CeT_3B_n ($T=\text{Ag, Pd, Rh, Ru}$; $n=0, 1, 2$) compounds, Perez *et al.*¹⁹ found a similar result. Namely, they observed that a collapse of the Ce-valence data plotted versus d -electron count for these three ($n=0, 1,$ and 2) systems could be achieved provided the effective B contribution to the $T(4d)$ band be fixed at the same two electrons per B found above. As will be emphasized below, however, both band filling and the formation of bonding and antibonding states play major roles in the alteration of the states in these ternary compounds.

b FEATURE AND Pd-B BONDING

We return now to the shift in spectral intensity into the higher-energy b feature with increasing B content in the $\text{Pd}_{1-x}\text{B}_x$, $x > 0.3$ series of compounds. To illustrate this effect we show in Fig. 4(a) a comparison of the Pd L_3 spectra of Pd and $\text{Pd}_{0.6}\text{B}_{0.4}$, and referring back to Fig. 3 note the difference of these two spectra. Both of these figures clearly show the loss of spectral intensity near E_F and its increase at higher energy. Although the subtraction method of Fig. 3 leaves some uncertainty, it would appear that the loss of a feature intensity has saturated by $x=0.1$ and that the development of intensity in the b feature dominates the spectral changes with x for $x > 0.1$.

Our interpretation of these results follows the spirit of the band-structure calculations of Gelatt, Williams, and Moruzzi¹⁸ for PdB, whose density-of-states (DOS) predictions are shown in Fig. 5 along with the DOS for elemental Pd from Papaconstantopoulos.²³ The work of Bakker *et al.*¹⁷ and Gelatt, Williams, and Moruzzi¹⁸ emphasized the importance of strong Pd(d)-B hybridization leading to the splitting off of bonding and antibonding states be-

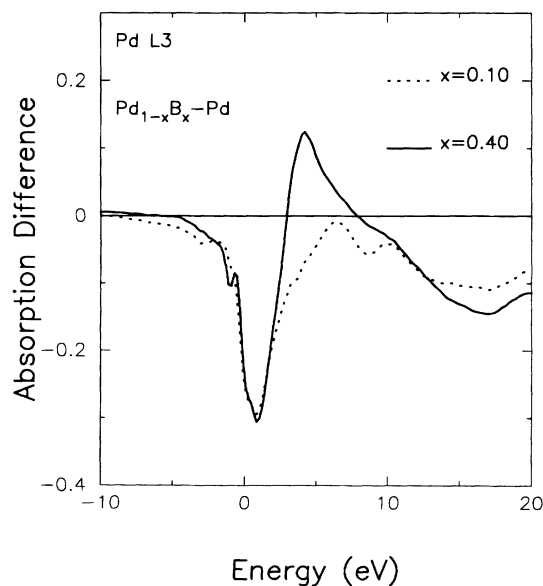


FIG. 3. Pd L_3 difference spectrum obtained by subtracting the elemental spectrum from that of the $x=0.1$ and 0.4 , $\text{Pd}_{1-x}\text{B}_x$ materials.

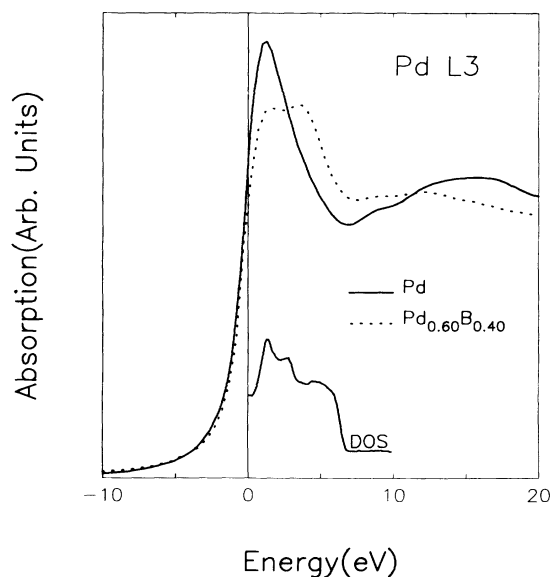


FIG. 4. Comparison of the Pd L_3 spectra of elemental Pd and the compound $\text{Pd}_{0.6}\text{B}_{0.4}$. The above E_F DOS prediction of Gelatt, Williams, and Moruzzi (Ref. 18) is also shown.

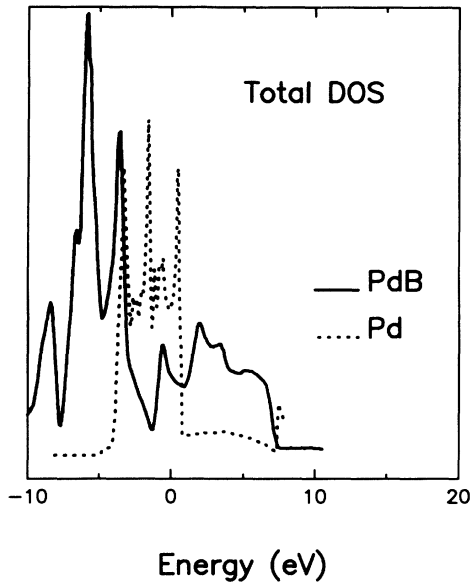


FIG. 5. Comparison of the predicted DOS for PdB [Gelatt, Williams, and Moruzzi (Ref. 18)] to that for elemental Pd [Papaconstantopoulos (Ref. 23)].

tween 3 and 10 eV above and below the nonbonding Pd- d states. The strong decrease in E_F states (relative to Pd) and the appearance of antibonding states up to 7 eV above E_F particularly should be noted. Gelatt, Williams, and Moruzzi's DOS results¹⁸ are also displayed in Fig. 4(a) along with the Pd L_3 spectra to illustrate the fact that DOS structure on an energy scale comparable to that of the b feature does exist. We associate the b feature with transitions involving the Pd-site- d -projection of antibonding Pd- d /B states that have been shifted well above E_F . We will now turn to a series of ternary intermetallic compounds in which similar $4d$ -state restructuring appears operative.

RT_3B_n COMPOUNDS

A large number of rare-earth (R) compounds of the form with the formula RT_3B_n with $T = \text{Ru, Rh, Pd, Ag}$, and $0 \leq n \leq 1, n = 2$, and $n = 3$. Here the RT_3 compounds are in the cubic AuCu_3 structure, and the RT_3B_n ($0 \leq n \leq 1$) are in the same structure with the B occupying the body-centered hole. The RT_3B_2 occurs in a hexagonal structure.¹⁹ We now wish to address the role that B coordination plays in modifying the $4d$ orbitals in these series of compounds.

The motivation for studying the Pr based PrRh_3B_n ($n = 0, 2, 3$) series of compounds is threefold. Namely, the Pr series supports all three crystal structures, potential confusion with La- $4f^1$ shakedown effects²⁴ are avoided, and potential variable valence Ce effects are avoided. In fact, similar effects have been identified in a number of other compounds; however, discussion of these will be deferred to a later paper.

In Figs. 6(a) and 6(b) we show the Rh $L_{2,3}$ spectra of a series of PrRh_3B_n compounds. These results show a

number of strong similarities to our Pd-B results above, and our discussion will proceed analogously. We identify an E_F a feature and a higher energy b feature. We note that the $n = 0$ compound exhibits a stronger a feature than the B containing materials. As before, we associate this with a decrease of $4d$ states near E_F upon B compounding. We note also that the b feature first appears between the $n = 0$ and $n = 1$ compounds, and is strongest and/or best resolved in the $n = 2$ compound. In the case of the $n = 1$ compound the excess intensity in the region of the b feature is spread over a rather broad range. As above, we associate the excess intensity in these features with antibonding Rh- $4d$ /B states shifted well above E_F .

In Fig. 7 we show the Rh L_2 spectrum of the $n = 2$ compound in this series, along with the projected Rh

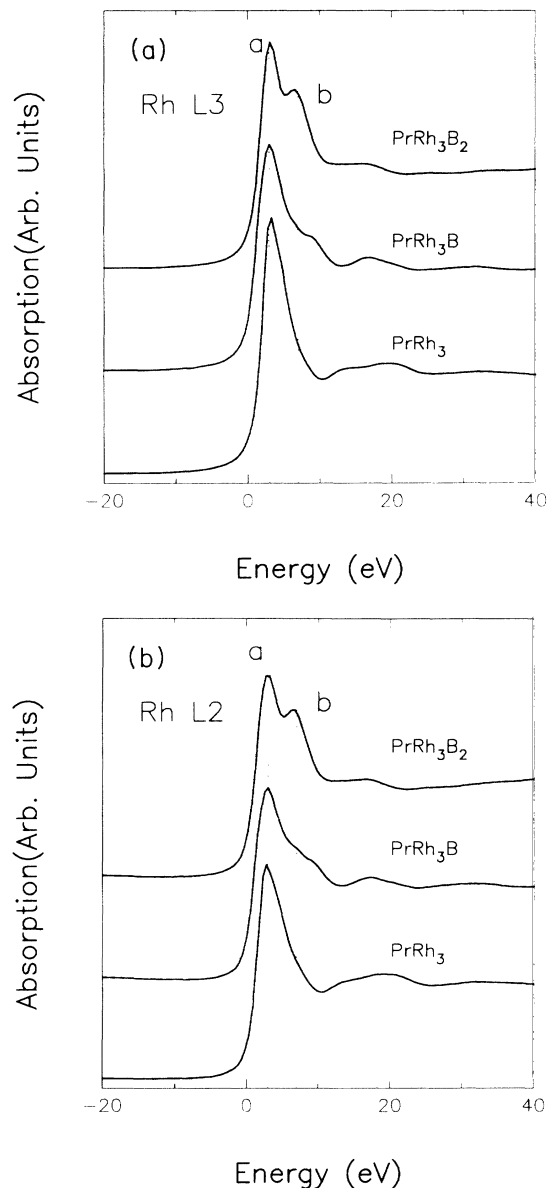


FIG. 6. Rh L_3 (a) and L_2 (b) spectra for PrRh_3B_n , $n = 0, 1, 2$ series of compounds.

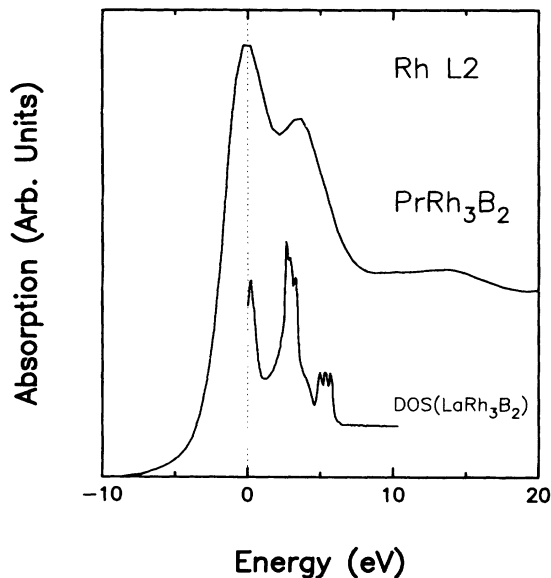


FIG. 7. Rh L_2 spectrum of PrRh_3B_2 . The Rh sphere, d -symmetry projected DOS prediction of Takegahara, Harima, and Kasuya (Ref. 25) is also shown.

sphere, d density of states from the band-structure calculations of Takegahara, Harima, and Kasuya.²⁵ The point to be emphasized here is that for this compound there is indeed sharp structure in the Rh- d state DOS at an energy close to the observed b feature. Thus it appears that the $T(4d)$ -B hybridization in these ternary compounds proceeds similarly to the Pd-B compounds noted above.

It is important to attempt to correlate site-specific XAS information gathered on different sites into an overall picture of the electronic structure of a series of materials. Therefore we would like to return to consider the Ce-valence-instability observations made by Perez *et al.*¹⁹ for these RT_3B_n series of materials. Although those observations were couched in terms of an effective T -sublattice electron count (*vid infra* in a rigid band), the present results suggest that it might be more appropriate to consider the movement of the Fermi energy in a d band that definitely changes. The simple addition of electrons to a rigid d band would lead to an increase in E_F , thus the d -electron-addition observation of Perez *et al.* is equivalent to a B-addition induced increase in the E_F within the d band. If, on the other hand, a T -B bonding interaction shifts d states from well below to well above

the Fermi energy, an increase in the Fermi energy of the d band would be required to accommodate the same number of d electrons despite the loss of low-energy states. In terms of the d -band Fermi energy movement, therefore, simple electron addition and antibonding state formation can induce qualitatively similar increases. Thus our T -sublattice results are reconcilable with the Ce-sublattice results of Perez *et al.* provided the Ce-valence response is viewed as coupled to the T - d -band Fermi energy rather than simply the d -electron count.

SUMMARY AND CONCLUSION

This work has presented systematic XAS studies of the $T(4d)$ - $L_{2,3}$ WL features of selected $4d$ -row elements and compounds. Based on these studies a number of XAS and electronic proposals have been advanced as summarized below.

A new linear coupling between the $L_{2,3}$ WL feature strength and the $4d$ -hole count in the $4d$ elements Mo to Ag has been observed and the utility of applying this result to compound studies has been emphasized. For low B concentrations in the interstitial $\text{Pd}_{1-x}\text{B}_x$ alloy, the Pd- $L_{2,3}$ WL area was found to decrease at a rate consistent with two Pd- d holes being filled per B substituted (here the elemental WL area to d -hole coupling was useful in quantifying this rate). For $\text{Pd}_{1-x}\text{B}_x$ ($x > 0.2$) compounds the WL area decrease (noted for the aforementioned alloys) was seen to saturate and a split-off WL feature to grow in intensity with increasing B content. We have interpreted these split-off features as reflecting antibonding states with admixed Pd- d character, after the theoretical work of Gelatt, Williams, and Moruzzi. Finally, we have found a similar but more robust split-off WL feature effect in the Rh $L_{2,3}$ spectra of a series of PrRh_3B_n ($n=0,2,3$) compounds. In these compounds we have again suggested that the formation of Rh(d)-B antibonding states split above E_F are responsible for these spectral changes.

Electronic structure calculations, specifically addressing the $T(4d)$ - $L_{2,3}$ absorption edge features, for the compounds studied here are clearly motivated by our results. Additional spectroscopic studies probing the $T(4d)$ sphere electronic structure in these materials would be useful. Finally, additional work is needed toward integrating electronic structure information as viewed from multiple lattice sites (e.g., the Ce sublattice work of Perez *et al.* and the present T -sublattice work) with spectroscopies that integrate over all sites (e.g., direct and inverse photoemission).

¹J. Horsley, J. Chem. Phys. **76**, 1451 (1982).

²L. Matthes and D. Dietz, Phys. Rev. B **22**, 1663 (1980).

³E. Stern and J. Rehr, Phys. Rev. B **27**, 3351 (1982).

⁴F. Lytle, J. Catal. **43**, 376 (1976).

⁵F. Lytle, P. Wei, R. Gregor, G. Via, and J. Sinfelt, J. Chem. Phys. **70**, 4849 (1980).

⁶M. Brown, R. Peierls, and E. Stern, Phys. Rev. B **15**, 738 (1977).

⁷B. Qi, I. Perez, P. Ansari, F. Lu, and M. Croft, Phys. Rev. B **36**, 2972 (1987).

⁸I. Perez, B. Qi, G. Liang, F. Lu, M. Croft, and D. Wieliczka, Phys. Rev. B **38**, 12 233 (1988).

⁹Y. Jeon, B. Qi, F. Lu, and M. Croft, Phys. Rev. B **40**, 1538 (1989).

¹⁰T. Sham, Phys. Rev. B **31**, 1888 (1985).

¹¹T. Sham, Phys. Rev. B **31**, 1903 (1985).

- ¹²M. DeCrescenzi, E. Colavita, U. Del Pinnino, P. Sassaroli, S. Valeri, C. Rinaldi, L. Sorba, and S. Nannarone, *Phys. Rev. B* **32**, 612 (1985).
- ¹³O. Bisi, O. Jepsen, and O. Andersen, *Phys. Rev. B* **36**, 9439 (1987).
- ¹⁴K. Allard, T. Flanagan, and E. Wicke, *J. Phys. Chem.* **74**, 298 (1970).
- ¹⁵H. Husemann and H. Brodowsky, *Z. Naturforsch. Teil A* **23**, 1693 (1968).
- ¹⁶M. Mahnig and L. Toth, *Phys. Lett.* **32A**, 319 (1970).
- ¹⁷H. Bakker, W. Joss, R. Griessen, L. Huisman, and H. Brodowsky, *Phys. Rev. B* **31**, 1729 (1985).
- ¹⁸C. Gelatt, A. Williams, and V. Moruzzi, *Phys. Rev. B* **27**, 2005 (1985).
- ¹⁹I. Perez, G. Liang, J. Zhou, H. Jahns, S. A. Shaheen, and M. Croft, *Physica B* **163**, 618 (1990).
- ²⁰T. Guo and M. den Boer, *Phys. Rev. B* **31**, 6233 (1985).
- ²¹J. Chen, Ph.D. thesis, Rutgers University, 1992.
- ²²See *Constitution of Binary Alloys, First Supplement*, edited by R. Eliot (McGraw-Hill, New York, 1965), p. 129.
- ²³D. Papaconstantopoulos, *Handbook of the Band Structure of Elemental Solids* (Plenum, New York, 1986).
- ²⁴A. Bianconi, A. Marcelli, I. Davoli, S. Stizza, and M. Campagna, *Solid State Commun.* **49**, 409 (1984).
- ²⁵K. Takegahara, H. Harima, and T. Kasuya, *J. Phys. Soc. Jpn.* **54**, 4743 (1985).